

MULTIMODAL REGISTRATION OF INTRAVASCULAR ULTRASOUND IMAGES AND ANGIOGRAPHY

David Rotger, Petia Radeva

Universitat Autònoma de Barcelona
Centre de Visió per Computador
Bellaterra, Spain

Eduard Fernández-Nofrerías, Josepa Mauri

Hospital Universitari Germans Trias i Pujol
Hemodinamics
Badalona, Spain

ABSTRACT

The growing appreciation of the pathophysiological and prognostic importance of arterial morphology has led to the realization that angiograms are inherently limited in defining the distribution and extension of coronary wall disease. By intravascular ultrasound (IVUS) images physicians have a picture of the composition of vessel in detail. However, observing an IVUS stack of images, it is difficult to figure out the image position and extension with regard to the vessel parts and ramifications, and misclassification or misdiagnosis of lesions is possible. The objective of this work is to develop a computer vision technique to fuse the information from angiograms and IVUS images defining the correspondence of every IVUS image with a point of the vessel in the angiograms by making a 3D reconstruction of the IVUS catheter's path from its projection in the angiography and placing there the IVUS planes.

1. INTRODUCTION

According to the American Heart Association coronary heart disease (CHD) caused 459,841 deaths in the United States in 1998 (1 of every 5 deaths) and in 1999 they estimated 61,800,000 Americans have one or more forms of cardiovascular disease (CVD) [1]. This figure is easy to extrapolate to the most of the developed countries along the western world. In Spain, more than the 90% of the sudden deaths have a cardiac origin resulting in more than 20,000 each year. CHD is still the first death cause in 2002 (up to 130,000 deaths per year, the 40% of the global mortality) [2].

1.1. Angiography vs IVUS

The main difference between the ultrasound and the angiography images, as the most used image modalities for vessel diagnosis, deals with the fact that the most of the visible plaque lesions with IVUS are not evident with angiogram (the silhouette of an angiographic image depends on the viewing angle) which often leads physicians to underestimate the extent and severity of the plaque in the artery. This problem is solved with IVUS due by providing a transverse, cross-sectional view of the vessel.

1.2. Models of vessel

One of the problems of dealing with IVUS is the fact that the images represent a 2D plane perpendicular to the catheter without any depth information. IVUS image is to artery as the face of a slice of bread is to the loaf. This IVUS property hides the real disease's extension and represents a very unnatural way of conceptualization. The foremost limitation of IVUS on the pre- and post-treatment studies is the need of correlating lesion images in

serial studies. This limitation is due to the lack of third dimension that gives much more global information about the internal and external vessel structure. Nowadays, the only way of determining the extension of a lesion and its position in respect to a certain bifurcation or a point evident in the angiography is by the use of the time stamp on the IVUS images. The precision of these calculus is very low (1 second \equiv 0.5-1.0 mm).

The widely recognized potency of deformable models stems from their ability to segment, match and track images of anatomic structures by exploiting (bottom-up) constraints derived from the image data together with (top-down) *a priori* knowledge about the location, size and shape of these structures.

1.3. Our goal

The correlation problem of the IVUS images can be solved by using the information given by the angiographies (shape and tortuosity: overall map of the vessel). Using two angiogram projections in fixed angles and taking into account the calibration parameters of the acquisition system, we are able to create a curve model in the space representing the catheter path during its pullback. This will give a more realistic idea of the vessel shape given that we will solve the problems coming from the viewing angle like the foreshortening effect or lesion underestimation.

This curve model of the vessel is not enough in order to determine the location and distribution of the lesion. It is necessary to fuse this information of the external vessel shape with the internal information coming from the IVUS images in order to give a more realistic way of conceptualization of the pathologies. Models of the internal layers of the vessel can be created by analyzing the IVUS images. If we are able define exact correspondence between data coming from both image modalities, that is to place IVUS images along the vessel curve, we will also be able to place the models of the internal layers coming from the IVUS images around the curve giving a realistic view of the vessel shape and tortuosity and a way of easier the correlation problem.

The article is organized as follows: section 2 is devoted to the catheter segmentation in angiograms. Section 3 explains the 3D reconstruction of the segmented catheter path and the images acquisition protocol. Section 4 discusses the process of fusing IVUS and angiography information. Section 5 explains the validation process and the obtained results. The article finishes with conclusions.

2. CATHETER SEGMENTATION

Intravascular ultrasound images are acquired during a catheter pullback through the vessel. Using an angiogram-guided process, the catheter is introduced in the vessel to diagnose, and positioned after the vessel lesion. Afterwards, a pullback with constant speed is performed acquiring the IVUS images. Therefore, the obtained stack or sequence of images define a spatio-temporal data that allow to scan the morphology of the vessel lesion in space.

In order to locate IVUS images in space we need an 3D reconstruction of the catheter trajectory. To this purpose, we need to register the catheter in two views of angiograms before and after the pullback of the IVUS catheter. Moreover, to assure precise 3D reconstruction of the catheter from both X-ray views, minimal spatial displacement of the catheter should occur during the process of acquisition of multiple views of X-ray images. A biplane X-ray system provides two views of the catheter at the same time that yield better conditions for a precise 3D reconstruction of the catheter. However, today many hospital environments are equipped with mono-plane X-ray devices. Considering the general case, given a mono-plane X-ray image system, we use ECG-gated X-ray images and the patient is asked to keep its breathing during an instant X-ray image acquisition in order to keep minimal spatial displacement of the catheter (a more extensive explanation of the acquisition protocol could be seen in section 3).

2.1. Local enhancement

Given that X-ray images are characterized with low signal-to-noise rate, an image enhancement step is necessary in order to improve the visualization and the performance of the following processing algorithms. We perform a histogram-based local image enhancement of X-ray images defined as follows:

$$\begin{aligned} I(x, y) &= \frac{I(x, y) - a}{(b - a)}, \\ a &= \min_{x', y' \in N(x, y)} I(x', y'), \\ b &= \max_{x', y' \in N(x, y)} I(x', y') \end{aligned} \quad (1)$$

where $N(x, y)$ is a neighborhood of pixel (x, y) of fixed size.

2.2. Catheter path reconstruction

The reconstruction of the whole trajectory of the catheter contains 2 steps: a) detection of the catheter projection in two views, and b) reconstruction of its trajectory in space. At this stage, the physician is asked to locate the end of the catheter before and after the pullback in both views of angiograms helped by the epipolar line (see fig. 1) and two 3D points are reconstructed. Note that these points represent the center of first and last IVUS images. Spatial reconstruction process of an 3D point from its projections is explained in section 3.

The process of catheter detection consists of applying the *fast marching algorithm* presented by Cohen and Kimmel [3] that allows to find a path with minimal geodesic distance between two points of an image. It is a segmentation algorithm based on the level set theory. A surface of minimal action (SMA) is constructed as a level set of curves L where the level corresponds to the geodesic distance $C\{L\}$ from an initial point A (p_0). Thus, each point, p from the SMA, U_0 (SMA with initial point p_0) has a value $U_0(p)$ equal to the integral minimal energy of the geodesic path P starting from the initial point p_0 and ending at point p :

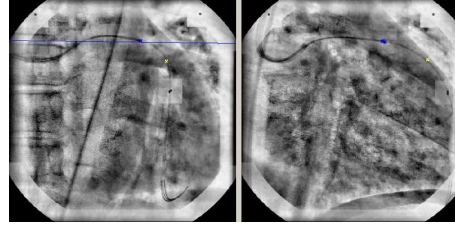


Figure 1. Localization of catheter head before and after IVUS pullback.

$$U_0(p) = \inf_{C\{L\}=p} \int \tilde{P} ds \quad (2)$$

Here, there is an iterative resolution of the Fast Marching algorithm:

Initialization:

- For each point of the grid, let $U_{i,j} = \infty$ (large positive value). Label all points as *far*.
- Set the start point $(i, j) = p$ to be zero: $U_p = 0$, and label it *trial*.

Marching Forward Loop:

- Let (i_{min}, j_{min}) be the *trial* point with smallest U value.
- Label the point (i_{min}, j_{min}) as *alive*, and remove it from the *trial* list.
- For each of the 4 neighboring grid points (k, l) of (i_{min}, j_{min}) :
 - If (k, l) is labelled *far*, then label it *trial*.
 - If (k, l) is not *alive*, then compute the $U_{k,l}$, selecting the largest solution (u), which is the only valid solution.

In order to determine the minimal path between p_0 and p_1 , we need only to calculate U_0 and then slide back on the surface U_0 from $(p_1, U_0(p_1))$ to $(p_0, 0)$. The surface of minimal action U_0 has a convex like behavior in the sense that starting from any point $(q, U_0(q))$ on the surface, and following the gradient descent direction on U_0 ($\frac{\partial C}{\partial \sigma} = -\nabla U_0$), we will always converge to p_0 . It means that U_0 has only one local minimum that is of course the global minimum and is reached at p_0 with value 0 (see fig. 2).

As a result, considering two projections with the catheter stopped before the pullback begins and another two at the end, we create a curve model of the pullback situating one model's extreme at the position of the IVUS catheter before the pullback begins and, using the projections taken at the end of the pullback, situate the ending extreme of the model coinciding with the last position of the catheter during its pullback.

3. 3D RECONSTRUCTION OF IVUS CATHETER FROM ANGIOGRAMS

Given that our aim is to measure the catheter length in order to place IVUS images along its trip inside the blood vessel, we need a three-dimensional reconstruction of this trip in order to minimize the *foreshortening* effect (the process of applying linear perspective to a figure).

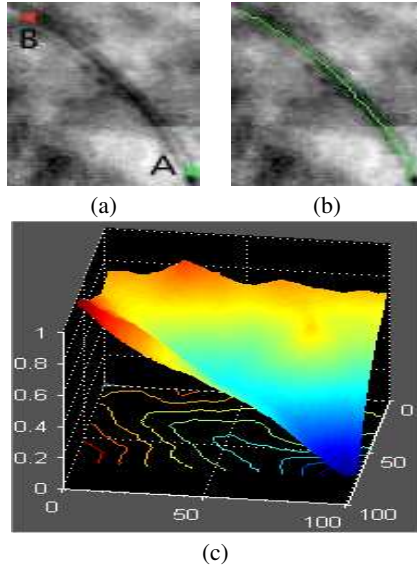


Figure 2. (a) Preprocessed X-ray image, (b) geodesic path between points A and B and (c) surface of minimal action

Our next goal is to create a three-dimensional global reference system where all the information coming from the two projections of the catheter is related to generate a unique model of the catheter in the space coming from the back-projection of the models segmented in the angiographies. To this propose, we have followed the steps proposed by Dumay et. al. in [4].

To assure minimal error in the reconstruction of the catheter path, we have proposed an acquisition protocol consisting in the following steps:

1. Choose two *optimal views* (minimum foreshortening) of the catheter with an angulation between both projections greater than or equal to 30 degrees, avoiding to change the distance between the intensifier and the isocenter (CF).
2. Acquire the first projection with the catheter stopped at the beginning of the pullback, asking the patient to keep the breathing to avoid displacement during the sequence.
3. Acquire the second projection without changing the CF and avoiding to use saved positioning (great mechanical error).
4. Do the pullback of the IVUS catheter without moving the C-Arm.
5. Acquire two more projections with the catheter stopped and the pullback's end following steps 3 and 2.

Given that there is significant displacement along the sequence due to the heart movement, we use the ECG of the angiograms to synchronize the images with the cardiac cycle choosing only the ones corresponding to the same position of the heart during a beat (the ECG R-wave).

Once both projections of the catheter have been obtained and segmented, M equidistant points from the segmentation model of one of the projections are chosen. It is easy to show that their corresponding points are the intersections of the corresponding epipolar lines and the detected catheter projection in the other X-ray view. Once defined the corresponding points from both angiograms, their 3D points are reconstructed and interpolated by a spatial B-spline curve [5] that represents the 3D reconstruction of the catheter path done between the beginning and the end of the pullback (see fig. 2). Note that this spatial curve represents the trace of the centers of the IVUS images.

4. MULTIMODAL IMAGE FUSION

4.1. Pullback phases

The task of registering IVUS data with angiogram information transforms to situating the IVUS images along the reconstructed 3D curve. After some unsuccessful attempts, and thanks to the use of a transparent phantom, we noticed that, even though using an automatic catheter pullback of constant speed (0.5mm/s), the transducer did not start its movement immediately after it was switched on; otherwise, it described different phases once the pullback has been switched on: Delay Before pullback (DB), Positive Acceleration phase (PA), phase of Constant Movement of the catheter (CM) and Negative Acceleration phase (NA). Further explanations on how the cycles have been estimated and the results obtained can be seen in section 5.

DB vary a lot depending on the length of the catheter inserted and its tortuosity of its journey along the vessel, but PA and NA delays are very short (near to zero) what made us start positioning the last IVUS image at the curve's extreme, corresponding to the ending of the pullback, perpendicular to the curve and go on situating the other images along the curve at a distance given by the pullback speed and the images discretization. To this purpose, we have to calculate the normals and binormals of the 3D curve. Given that we are using B-Splines, we can analytically calculate the Frenet triangle $(\vec{t}, \vec{n}, \vec{b})$, where \vec{t} is the curve tangent, \vec{n} is the curve normal and \vec{b} is the curve binormal of the B-spline catheter model. We take into account that the IVUS image plane is perpendicular to the catheter that means that coincides with the perpendicular plane defined by the normal and binormal of the catheter model. Thus, taking into account the distance the catheter's head has moved from the end point of the catheter model (computed from IVUS data) and the 3D length of the catheter model (computed from the angiograms data), we can locate the IVUS plane in space.

4.2. IVUS images placement along the curve

Given that we are using B-Splines, we will use Blending function's formulae[5]. Let $Q(u)$ to be the B-Spline curve with internal parameter u .

The tangent (\vec{t}) and the normal (\vec{n}) vectors at $Q(u)$ are defined as:

$$\vec{t} = Q'(u), \quad \vec{n} = Q''(u)$$

To make \vec{t} and \vec{n} orthonormal:

$$\vec{n} = (\vec{t} \times \vec{n}) \times \vec{t}$$

And so the binormal vector is defined as:

$$\vec{b} = \vec{t} \times \vec{n}$$

So using $Q(u)$ we are able to calculate the position of any point of the curve in the space by using the appropriate \vec{v} and incrementing the internal variable u . If the increments of u are small enough we can calculate the length of a segment of the curve by accumulating the calculus of the Euclidean distance between all the consecutive points of the segment:

$$l = \sum_i \|Q(u_{i+1}) - Q(u_i)\|$$

where $(u_{i+1} - u_i) \mapsto 0$ and $u_i \in [0, 1]$.

When this distance is equal to or greater than the distance between two IVUS images, we will place there the center of the next IVUS plane orienting its vertical axis by \vec{n} and the horizontal one by \vec{b} .

The use of the triangle of Frenet creates an artificial rotational effect of IVUS planes around the tangent direction of the catheter. In order to minimize the rotational transformation between two consecutive planes, we project the normal and bi-normal vectors of the previous IVUS plane to the actual one, applying the following formulae:

$$\begin{aligned}\vec{n}_i &= \vec{n}_{i-1} - \vec{t}_i * (\vec{n}_{i-1} \cdot \vec{t}_{i-1}) \\ \vec{b}_i &= \vec{t}_i \times \vec{n}_i\end{aligned}$$

4.3. Correspondences

Once placed all IVUS images along the 3D curve of the catheter model that is described during the catheter pullback, we can determine the correspondence between IVUS and angiogram data. This fact allows to the user to define corresponding data between angiograms and IVUS data. Note that this fact is very important since angiograms give information about the external view of the vessels, distance to ramifications, lesions, stents and other anatomic parts of the hearts, while IVUS images provide information about the internal shape of the vessel e.g. its morphological structure, vessel wall thickness and composition, plaque, calcium deposits, etc

5. VALIDATION AND RESULTS

In order to validate the fusion algorithm, we have used two groups of test: *in-vitro* and *in-vivo*. The first group took us to the realization that the catheter movement describes different phases, as we have mentioned. This fact has to be considered in order to achieve a good registration between IVUS and its reconstructed catheter's path. We performed 13 pullback image acquisition on an IVUS phantom proportioned by Boston Scientific to estimate the mean and standard deviation of pullback phases measurements (see table 1).

Phase	Mean	Std.
DB	5.23s(2.62mm)	0.27s(0.14mm)
PA	0.27s(0.14mm)	0.19s(0.10mm)
CM	1.00s(0.50mm)	0.20s(0.10mm)
NA	0.02s(0,01mm)	0.62 (0.31mm)

Table 1. Mean and std of different phases of catheter movement.

Considering this fact, we defined a new acquisition protocol for the catheter and IVUS images yielding what we have called *Double Pullback*(DP), that consists in performing a short pullback assuring the transducer movement, before the first pair of projections are taken. 7 more pullbacks were performed using the DP technique to estimate the position of a calcium deposit, obtaining a mean error of 3mm (std. $\sigma = 0,42mm$).

We have also tested the system with 12 real cases of patients in the Hospital Universitari "Germans Trias i Pujol." of Badalona. We have reconstructed the catheter paths for these 12 pullbacks and measured their lengths. We have compared the obtained length with the one coming from the number of IVUS images it generated. 9 of these pullbacks were performed using the DP technique. Fig. 3 presents their regression line. The obtained mean error for this cases was 1,26mm (std. $\sigma = 0,9mm$). This error is confirmed by the physician team as acceptable to the purposes of lesion localization.

6. CONCLUSIONS

Fusing IVUS and angiogram data is of high clinical interest to help the physicians locate in IVUS data and decide which lesion is observed, how long it is, how far from a bifurcation or

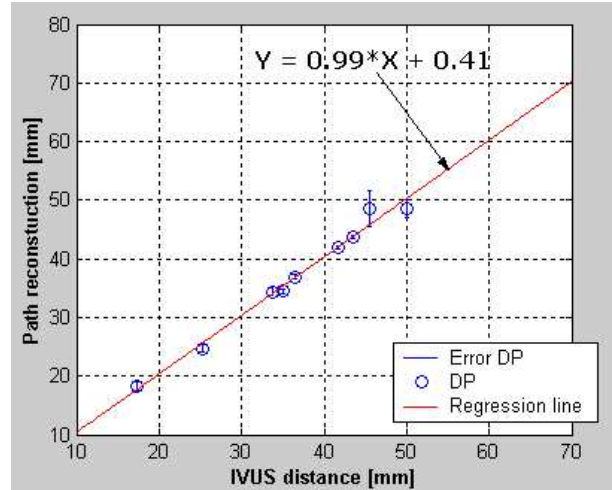


Figure 3. Path reconstruction vs IVUS distance (error and regression line)

another lesions stays, etc. We have introduced a semi-automatic technique (surface of minimal action) to detect the catheter path in the angiographies by determining the initial and final position of the transducer in two pairs of projections. A three-dimensional reconstruction method was implemented and studied, based on the work of Dumay et al. [4], to place this segmented catheter path in the space giving more information of its shape saving the foreshortening effect. The acquisition procedure has been studied deeply, fixing all the parameters and conditions to avoid ambiguity and make more precise the reconstruction, evaluated the contribution of each of the parameters to the final error, characterized the type of this error and its magnitude, leading to an accurate acquisition protocol. We have also stressed in simplifying the procedures and minimizing the cost in time and effort to assure the applicability of the described techniques. Moreover, we have introduced a new technique to determine exact correspondence between angiographies and IVUS images, based on the three-dimensional reconstruction of the catheter path. Going further on, we have characterized the different sources of error: mechanical (coming from the pullback device) and algorithmic, achieving the limit of the mechanical error.

7. BIBLIOGRAFÍA

- [1] "2001 heart and stroke statistical update," American Heart Association, <http://www.americanheart.org>, 2001.
- [2] Dr. Marin, "La cadena de supervivencia. aprende a salvar una vida," *Corazon y Salud, Fundación Española del Corazón*, vol. 23, pp. 3-9, July-September 2002.
- [3] Cohen and Kimmel, "Global minimum for active contour models: A minimal path approach," *International Journal of Computer Vision*, vol. 24, no. 1, pp. 57-78, August 1997.
- [4] Dumay, Reiber, and Gerbrands, "Determination of optimal angiographic viewing angles: Basis principles and evaluation study," *IEEE Medical Imaging*, vol. 13, pp. 13-23, 1994.
- [5] Barsky, Bartels, and Beatty, *An Introduction to Splines for use in Computer Graphics and Geometry Modeling*, Morgan Kaufmann Publishers INC, 1987.